



Research article

Exserolide J ameliorates lipid accumulation *in vitro* by regulating liver X receptor alpha and peroxisome proliferator-activated receptor alpha proteins

Yan Zhang^{a,1}, Xue Wang^{b,1}, Tian Liu^b, Zi-Yi Zhang^c, Wen-Gang Song^{d,**}, Shou-Dong Guo^{b,*}^a Department of Endocrinology and Metabolism, Guiqian International General Hospital, Guiyang, 550018, China^b Institute of Lipid Metabolism and Atherosclerosis, Innovative Drug Research Centre, School of Pharmacy, Shandong Second Medical University, Weifang, 261053, China^c School of Life Science and Technology, Harbin Institute of Technology, Harbin, 150001, China^d Shandong Provincial Key Laboratory for Rheumatic Disease and Translational Medicine, The First Affiliated Hospital of Shandong First Medical University & Shandong Provincial Qianfoshan Hospital, Jinan, 250014, China

ARTICLE INFO

Keywords:

Foam cell
Isotope tracing
LXR α agonist
Molecule docking
PPAR α agonist

ABSTRACT

Exserolides are isocoumarin derivatives containing lactone moiety. Recently, some isocoumarins have been demonstrated to ameliorate hyperlipidemia, a major factor for inducing cardiovascular diseases. However, the effects and mechanisms of action of exserolides on hyperlipidemia are not known. The aim of this study is to investigate whether the marine fungus *Setosphaeria* sp.-derived exserolides (compounds I, J, E, and F) exert lipid-lowering effects via improving reverse cholesterol transport (RCT) *in vitro*. RAW264.7 macrophages and HepG2 cells were used to establish lipid-laden models, and the levels of intracellular lipids and RCT-related proteins were determined by assay kits and Western blotting, respectively. We observed that exserolides (at a 5 μ M concentration) significantly decreased intracellular cholesterol and triglyceride levels in oxidized low-density lipoprotein-laden RAW264.7 cells and markedly improved [³H]-cholesterol efflux. Among the four tested compounds, exserolide J increased the protein levels of ATP-binding cassette transporter A1, peroxisome proliferator-activated receptor α (PPAR α), and liver X receptor α (LXR α). Furthermore, treatment with exserolides significantly decreased oleic acid-laden lipid accumulation in HepG2 hepatocytes. Mechanistically, exserolides enhance PPAR α protein levels; furthermore, compound J increases cholesterol 7 α -hydroxylase A1 and LXR α protein levels. Molecular docking revealed that exserolides, particularly compound J, can interact with PPAR α and LXR α proteins. These data suggest that the terminal carboxyl group of compound J plays a key role in lowering lipid levels by stimulating LXR α and PPAR α proteins. In conclusion, compound J exhibits powerful lipid-lowering effects *in vitro*. However, its hypolipidemic effects *in vivo* should be investigated in the future.

* Corresponding author. 7166[#] Baotongxi Street, Weifang, Shandong Province, China.

** Corresponding author. Jingshi Road 16766, Jinan, Shandong, 250014, China.

E-mail addresses: s.com@163.com (W.-G. Song), SD-GUO@hotmail.com (S.-D. Guo).¹ Contribute equally to this article.<https://doi.org/10.1016/j.heliyon.2024.e31861>

Received 8 January 2024; Received in revised form 22 May 2024; Accepted 22 May 2024

Available online 23 May 2024

2405-8440/© 2024 Published by Elsevier Ltd.

This is an open access article under the CC BY-NC-ND license

<http://creativecommons.org/licenses/by-nc-nd/4.0/>.

1. Introduction

Dyslipidemia is generally defined as elevated plasma levels of total cholesterol (TC), low-density lipoprotein (LDL) cholesterol or triglyceride (TG), or low levels of high-density lipoprotein (HDL) cholesterol (HDL-c) or a combination of these features [1]. Hyperlipidemia, as a kind of dyslipidemia, is primarily characterized as hypercholesterolemia and/or hypertriglyceridemia. In recent years, the prevalence of dyslipidemia and hyperlipidemia maintains at a high level globally. For instance, the prevalence of hypercholesterolemia, high LDL cholesterol, hypertriglyceridemia, and low HDL-c is found to be 18.8 %~29.2 %, 19.2 %~30.2 %, 31.1 %~41.8 %, and 29.3 %~53.9 %, in different areas of India [2]. The prevalence of dyslipidemia, hypercholesterolemia, hypertriglyceridemia, high LDL cholesterol, and low HDL-c is 39.3 %, 9.8 %, 19.6 %, 14.9 %, and 17.5 % in Xinjiang province of China, as revealed by a recent study [3]. Research has demonstrated that hyperlipidemia, particularly LDL cholesterol, are the primary risk factors for atherosclerosis, a basic pathological change of cardiovascular diseases (CVDs) [4]. Mechanistically, hyperlipidemia results in atherosclerosis by promoting the formation and accumulation of lipid plaques in the arteries [4–6]. At present, statins remain the leading lipid-lowering drugs that primarily inhibit 3-hydroxy-3-methylglutaryl coenzyme A (HMG-CoA) reductase, which is involved in the synthesis of mevalonate, a sterol precursor. However, many studies have revealed that statins and other synthetic and commercially available drugs exhibit side effects including muscle-related adverse events (e.g. cramps, myalgia, weakness, and rhabdomyolysis) and cognitive side effects [7,8]. Although proprotein convertase subtilisin/kexin type 9 (PCSK9) inhibitors can lower cholesterol levels as an adjunct to statins [9], their actual effects on ameliorating CVDs need to be investigated using large-scale clinical data. Therefore, discovering and exploring innovative strategies for lowering lipid levels are continuously warranted [10].

Notably, reverse cholesterol transport (RCT) promotes the transport of lipids from peripheral cells, such as macrophage, to

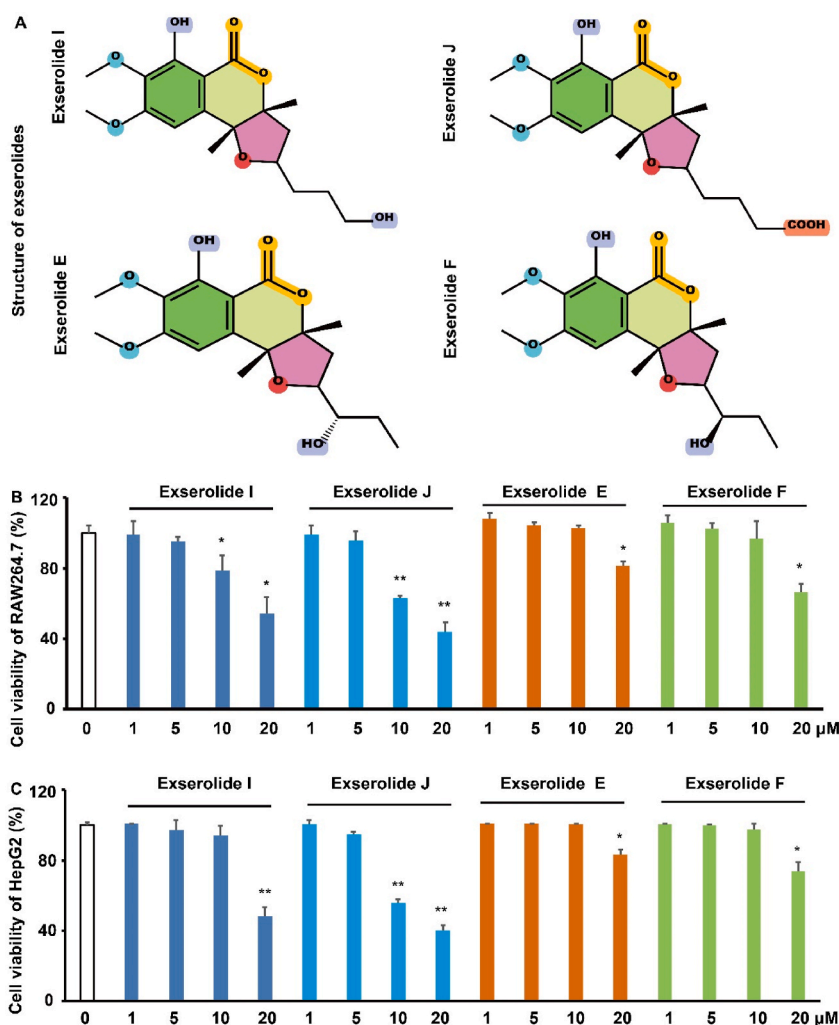


Fig. 1. Structure and cytotoxicity of exserolides ($n = 3$). A, structure of the four exserolides; B, cell viability of RAW264.7 macrophages in the presence of 0–20 μM exserolides; C, viability of HepG2 cells in the presence of 0–20 μM exserolides. * means $p < 0.05$ vs blank control; ** means $p < 0.01$ vs blank control.

apolipoprotein A1 and/or HDL particles in circulation via the liver X receptor (LXR) α -ATP binding cassette (ABC) A1 and/or ABCG1 signaling pathway. Next, plasma LDL particles and HDL particles are transported into liver for metabolism primarily by hepatic LDL receptor (LDLR) and scavenger receptor B type 1 (SR-B1), respectively [11]. In the liver, TGs are generally decomposed into fatty acids, which can be further catabolized primarily through peroxisome proliferator-activated receptor (PPAR) α -mediated β -oxidation; and cholesterol esters are decomposed into free cholesterol, which may be converted into bile acids via a series of enzymes, particularly cholesterol 7 α -hydroxylase A1 (CYP7A1) [12,13]. In the following, these lipid metabolites may be excreted from the liver via the LXR α -ABCG5/8 signaling pathways [14,15]. Notably, the RCT process has been demonstrated to attenuate hyperlipidemia as well as atherosclerotic CVDs in different models [6,11,16].

Owing to their novel structural characteristics and various biological activities, secondary metabolites from marine-derived microorganisms have garnered considerable attention [17]. Notably, fungi are a vital source for lipid-lowering drugs. For example, statins, a series of hydroxymethyl glutaryl CoA reductase (HMGCR) inhibitors, are originally isolated from the metabolites of *Penicillium citrinum* Pen-51 and *Aspergillus terreus* [18]. Exserolides are derivatives of isocoumarins, which are a class of distinctive fungal polyketides with various activities including antifungal, antibacterial, cytotoxic, anti-inflammatory, and enzyme-inhibitory activities [19,20]. Interestingly, some natural polyketides are found to improve the expression of the cholesterol transporter ABCA1, suggesting their potential roles in treatment of hyperlipidemia, especially hypercholesterolemia [21]. The endophytic fungus *Neofusicoccum parvum* JS-0968-derived isocoumarin derivative, (3R)-5-hydroxymellein, exhibits attractive lipid-lowering and anti-atherosclerotic activities [22]. Compared to other isocoumarin derivatives, exserolides are rarely reported. In 2014, Li et al. isolated 6 exserolides with potential antifungal and antibacterial activities. In 2018 and 2023, Pang et al. isolated 6 exserolides in total from the *Callyspongia* sp. Sponge-derived fungus *Setosphaeria* sp. SCSIO41009; and these exserolides exhibited potential antifungal, antioxidant, and antiviral activities [23,24]. Recently, exserolides L and M are demonstrated to have no effects on inhibition of HMGCR activity based on a non-cellular model [24]. However, whether exserolides have lipid-lowering effects in lipid-laden cellular models and the underlying mechanisms of action are unclear. In the present study, we evaluated the lipid-lowering effects of four exserolides (Fig. 1A) in lipid-laden RAW264.7 macrophages and HepG2 cells and investigated their potential mechanisms of action via focusing on RCT-related proteins. Given molecular docking is useful for explaining ligand–protein interactions of interested compounds, we also applied this in-silico technique to clarify the potential mechanisms of action of these four exserolides [25,26].

2. Materials and methods

2.1. Materials

Macrophage cell line RAW 264.7 (SCSP-5036) and human hepatocellular carcinoma cell line HepG2 (SCSP-510) were purchased from the Cell Bank of Chinese Academy of Sciences (Shanghai, China). Oleic acid (01008) and Oil Red O (00625) were bought from Sigma-Aldrich (St. Louis, MO, USA). [3 H]-cholesterol was obtained from China Isotope & Radiation Corporation (Beijing, China). Liver X receptor (LXR) agonist TO901317 (293754-55-9) and fenofibrate (S1794) were purchased from Selleck (Shanghai, China). Cell Counting Kit-8 (CCK-8, CK04) and dimethyl sulphoxide (DMSO, 821D035) were purchased from Solarbio (Beijing, China). Dulbecco's modified Eagle's medium (DMEM, C11995500BT) and fetal bovine serum (FBS, 10270) were bought from Gibco (Gaithersburg, MD, USA). Radio Immunoprecipitation Assay (RIPA) lysis buffer was provided by Merck (3108491, Darmstadt, Germany). A mouse monoclonal antibody against ABCA1 (ab18180, 1:200), rabbit polyclonal antibodies against LXR α (ab3585, 1:200) and cluster of differentiation 36 (CD36, ab64014, 1:500), and rabbit monoclonal antibodies against SR-B1 (ab217318, 1:2000), ABCG1 (ab52617, 1:1000), and LDLR (ab52818, 1:1000) were bought from Abcam (Cambridge, MA, USA). Mouse monoclonal antibodies against sterol regulatory element-binding protein (SREBP)-1c (sc-13551, 1:100), SREBP-2 (sc-271616, 1:200), and peroxisome proliferator-activated receptor (PPAR) α (sc-398394) were purchased from Santa Cruz Biotechnology (Santa Cruz, CA, USA). A rabbit polyclonal antibody against CYP7A1 (TA351400, 1:1000) and a rabbit polyclonal antibody against ABCG8 (TA388255, 1:2000) were provided by OriGene (Shanghai, China). Mouse monoclonal antibodies against β -actin (66009-1-Ig, 1:5000) and glyceraldehyde-3-phosphate dehydrogenase (GAPDH) (60004-1-Ig, 1:5000) and a rabbit monoclonal antibody against PCSK9 (55206-1-AP, 1:500) were purchased from Proteintech (Chicago, IL, USA). Complete protease inhibitor (HY-K0011) was obtained from MedChem Express (NJ, USA). Secondary antibodies (CW0103S and CW0102S) were bought from CWBIO (Beijing, China). Enhanced chemiluminescence (ECL) kits (WBKLS0500) were purchased from Sigma-Aldrich (St. Louis, MO, USA). Total cholesterol (TC, 100000180) and TG (100000220) assay kits were obtained from Biosino Bio-technology and Science Inc. (Beijing, China). All reagents used in this study were of analytical grade.

2.2. Preparation of lipoproteins

After signing the informed consent form for blood donation, approximately 20 mL of blood was collected from a healthy volunteer by a professional physician. Based on a previously described method, lipoproteins were prepared through sequential ultracentrifugation [27]. Plasma density was orderly adjusted to 1.006 and 1.063 g/mL and put into a CS150FNX type ultracentrifuge (Hitachi, Japan, Serial No. 281131), followed by centrifugation at 400,000 \times g for 24 h to obtain upper layers containing very low-density lipoproteins and LDL particles, respectively. Oxidized LDL (ox-LDL) was prepared according to our previously described method [27]. Briefly, LDL (~10 mg/mL) was incubated with CuSO₄ (10 μ M) at 37 $^{\circ}$ C for 24 h. The reaction was terminated by adding 500 μ M ethylenediaminetetraacetic acid disodium salt. The obtained ox-LDL particles were dialyzed against phosphate-buffered saline (PBS, pH = 7.4) at 4 $^{\circ}$ C for 24 h, followed by filtration and storage at 4 $^{\circ}$ C until use within 2 weeks.

2.3. Cell culture

RAW264.7 macrophages or HepG2 cells were seeded in 25-cm² flasks and cultured in DMEM (containing 4.5 g/L D-glucose, L-glutamine, and 110 mg/L sodium pyruvate) supplemented with 10 % FBS, 100 U/mL penicillin, and 100 µg/mL streptomycin. Cells were grown in a humidified incubator with 5 % CO₂ at 37 °C. In general, the cell culture medium was exchanged every 2 days [27].

2.4. Cell viability assay

Cells were seeded into a 96-well plate at a density of 1.0×10^4 cells/well. Compounds were dissolved in DMSO, with 0.1 % being the final DMSO concentration in the cell culture media. Negative controls were prepared using DMSO at a final concentration of 0.1 % [28]. Cells were treated with 0.0, 1.0, 5.0, 10.0, and 20.0 µM exserolides for 24 h. The CCK-8 method was used to evaluate cell viability. Briefly, after drug intervention, 10 µL of commercially available CCK-8 solution was added. Cells were incubated for an additional 3 h. Then, the absorbance was measured at 450 nm using the SpectraMax i3x Multi-Mode Microplate Platform (Molecular Devices, San Jose, CA, USA).

2.5. Cholesterol efflux assay

The cholesterol efflux assay was performed as previously described [27,28]. Appropriate concentrations of [³H]-cholesterol and ox-LDL were preincubated at 37 °C for 30 min; thereafter, they were added to DMEM supplemented with 1 % FBS. The final concentrations of [³H]-cholesterol and ox-LDL were 1 µCi/mL and 100 µg/mL, respectively. [³H]-cholesterol loaded cells were cultured with 500 µL of DMEM containing supplemented with 1 % FBS in the presence or absence of exserolides (5.0 µM) or TO901317 (1.0 µM) for 4 h. To imitate the actual situation *in vivo*, plasma was used as the cholesterol acceptor. Finally, [³H]-cholesterol content was measured in the culture media and within the cells using the Tri-Carb 2810 TR type liquid scintillation counter (PerkinElmer, USA). The percentage of [³H]-cholesterol efflux was calculated using the following equation [27,28]. CPM is the abbreviation for counts per minute.

$$\text{Efflux\%} = [\text{CPM of media} / (\text{CPM of media} + \text{CPM of cell extract})] \times 100\%.$$

2.6. Determination of intracellular TC and TG levels

RAW264.7 macrophages were seeded into 6-well plates (1×10^6 cells/well) and incubated with ox-LDL (50 µg/mL) in DMEM for 24 h. Then, cells were treated with DMEM supplemented with 10 % FBS in the presence of 5 µM exserolides or 1 µM TO901317 for an additional 24 h. Cells were gently washed with PBS and treated with 0.2 mL of RIPA lysis buffer at 4 °C for 30 min, followed by heating at 70 °C for 10 min and centrifugation at 1500×g for 5 min to remove cellular debris [27–29]. Finally, commercially available assay kits were used to measure the TC and TG levels in the supernatant. The absorbance was measured at 505 nm using the SpectraMax i3x Multi-Mode Microplate Platform (Molecular Devices).

HepG2 cells were incubated with 0.5 mM oleic acid for 24 h. Then, they were treated with DMEM supplemented with 10 % FBS in the presence of 5 µM exserolides or 2 µM fenofibrate for an additional 24 h [27,28]. Thereafter, intracellular TC and TG levels were measured using the above-described methods.

2.7. Oil red O staining

After the intervention, cells grown on glass slides in 6-well plates were fixed with 4 % (w/v) paraformaldehyde at 25 °C for 30 min, followed by staining with freshly prepared oil red O solution (5 mg/mL in 60 % isopropanol) at 25 °C for approximately 1.0 h [28]. Lipid-stained cells were captured using the Axio Vert. A1 inverted microscope (Zeiss, Jena, Germany). Images were recorded on the AxioCam 506 color camera (Zeiss).

2.8. Immunoblotting

Total proteins were extracted using RIPA lysis buffer. Equal amounts of protein (approximately 50 µg) were subjected to 12 % or 10 % sodium dodecyl sulfate polyacrylamide gel electrophoresis and transferred onto polyvinylidene fluoride membranes via electroblotting. After blocking with 5 % defatted milk (dissolved in PBS-Tween20 solution), the membranes were horizontally cut to probe different target proteins before 2020. Thereafter, intact membranes were used to blot target proteins. The membranes were washed three times with PBS-Tween 20 solution and incubated with horseradish peroxidase-conjugated secondary antibodies for 2 h at 25 °C. An enhanced chemiluminescence reaction was used to analyze the immunoblots. Images were captured on the Clinx ChemiScope 6000 pro system (Shanghai, China). Densitometric analysis was conducted using Image J Software. Protein levels were normalized using the housekeeping protein β-actin or GAPDH [28].

2.9. Molecular docking

Molecular docking was performed using the DELL T5820 workstation along with Pymol and Autodock Vina software. The three-

dimensional (3D) crystal structures of LXR α (ID: 3IPQ) and PPAR α (ID: 1I7G) were obtained from the Protein Data Bank RCSB (<http://www.pdbus.org/>). Notepad was used to remove the ligand molecule linked to the downloaded LXR α or PPAR α protein–ligand complex. After adding a hydrogen atom and correcting the electric charge using AutoDock software, the 3D protein structures were retained for subsequent analysis. The active sites and parameters for molecule docking were determined based on the ligand and active pocket of the downloaded ligand–protein complex. The stable optimized conformation of exserolides was determined by minimizing the energy module using the MM2 molecular program. Chem3D software was used to convert the preferred conformation of exserolides to the mol2 format, which was then converted to the pdbqt format using Open Babel software. The central coordinate values and sizes of the GridBox for LXR α were 43.752, 26.263, and -0.676 , and 45.90, 55.65, and 46.80, respectively. The central coordinate values and sizes of the GridBox for PPAR α were 33.245, 27.154, and 30.800 and 47.60, 57.75, and 47.75, respectively. AutoDock Vina software combined with the Lamarckian genetic algorithm was used to search the conformation by focusing on the active center of LXR α or PPAR α protein. The maximum time for energy evaluation was 2,500,000. Protein-Ligand Interaction Profiler (PLIP) ([**Panel A: Oil Red O Staining**

RAW264.7 cells \(Oil Red O staining\)

Blank, oxLDL, oxLDL + TO, oxLDL + I, oxLDL + J, oxLDL + E, oxLDL + F

Panel B: Intracellular TC Levels

Group	TC \(\$\mu\text{g}/\text{mg}\$ protein\)
Blank	~1.2
Model	~3.0###
TO	~1.6***
I	~2.4*
J	~1.9**
E	~2.5
F	~2.4

Panel C: Intracellular TG Levels

Group	TG \(\$\mu\text{g}/\text{mg}\$ protein\)
Blank	~13
Model	~26###
TO	~21
I	~20*
J	~18**
E	~20*
F	~20*

Panel D: Cholesterol Efflux \(%\)

Group	Cholesterol efflux \(%\)
Vehicle	~10
TO	~20***
I	~13*
J	~14*
E	~12&
F	~13
</div>
<div data-bbox=)

Fig. 2. Effects of exserolides on lipid accumulation in ox-LDL-laden RAW264.7 macrophages ($n = 3$). Ox-LDL-laden RAW264.7 macrophages were treated with exserolides or LXR α agonist TO901317. A, typical pictures of oil red O staining; B, intracellular TC levels; C, intracellular TG levels; D, percentage of [^3H]-cholesterol efflux from macrophages to culture medium. TO: TO901317; I: exserolide I; J: exserolide J; E: exserolide E; F: exserolide F. The abbreviations are suitable for the rest figures. ### means $p < 0.01$ vs blank control; * means $p < 0.05$ vs model group; ** means $p < 0.01$ vs model group; & means $p < 0.05$ vs TO901317.

plip-tool.biotech.tu-dresden.de) was used to determine ligand–protein interactions such as hydrophobic contacts, salt bridges, and π -stacking according to a previous study [25,30]. Furthermore, root mean square deviation (RMSD) of the ligand–protein interaction was computed to determine the reliability of the molecular docking. In general, the docking approach is considered to be credible if $RMSD \leq 2 \text{ \AA}$ [31,32].

2.10. Data analysis

All bioassay results were expressed as mean \pm standard deviation for at least three independent experiments. Data normality was carried out using the SPSS software version 26. Paired Student-T-Test was used to perform statistical analysis. Differences were considered to be significant at a P -value of <0.05 .

3. Results

3.1. Cytotoxicity

We investigated whether exserolides from the fungus *Setosphaeria* sp. SCSIO41009 exert lipid-lowering effects *in vitro* and revealed the underlying mechanisms of action using fenofibrate and the LXR agonist TO901317 as positive controls in HepG2 cells and macrophages, respectively. Because higher levels of TO901317 and fenofibrate may induce cytotoxicity [27,28], the concentrations of TO901317 and fenofibrate were set at 1 and 2 μM , respectively. Fig. 1B (RAW264.7) and Fig. 1C (HepG2) illustrate that these compounds exhibited no significant cytotoxicity compared with the blank control within the concentration range of 0–5 μM . To obtain a potential maximum lipid-lowering effect without inducing cytotoxicity, 5 μM exserolides were used in the subsequent studies.

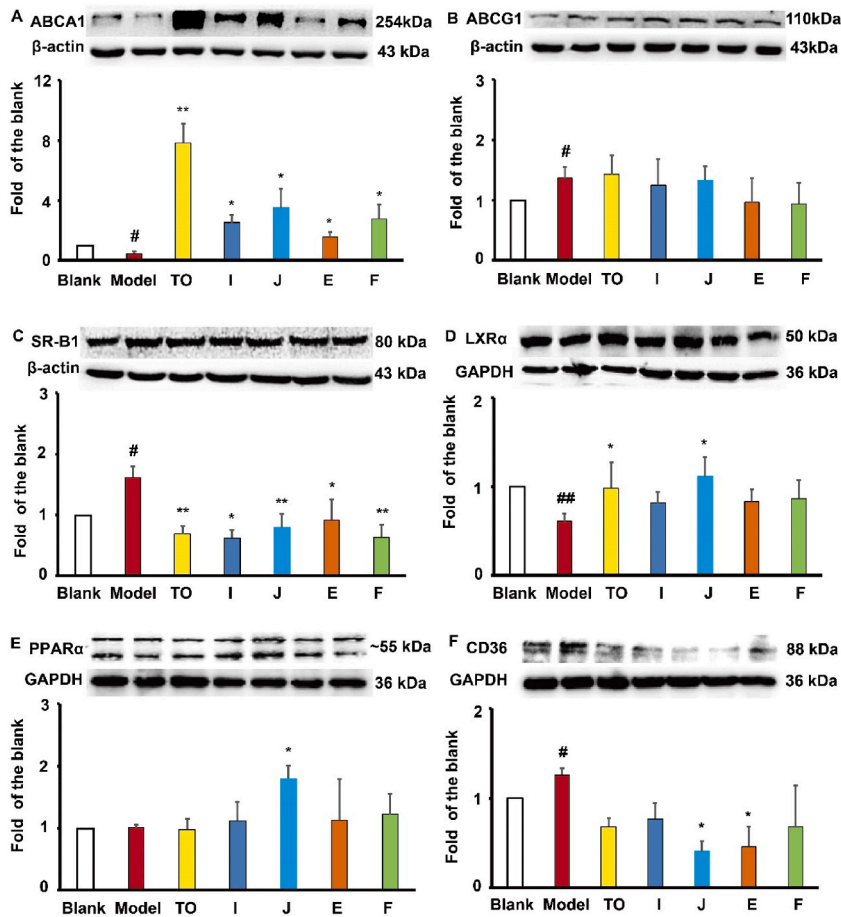


Fig. 3. Effects of exserolides on RCT-related protein levels in RAW264.7 macrophages. A, B, C, D, E, and F, ABCA1 (n = 3), ABCG1 (n = 4), SR-B1 (n = 3), LXRα (n = 3), PPARα (n = 3), and CD36 protein levels (n = 3), respectively. The raw images were provided as supplementary material for Fig. 3A–F. # means $p < 0.05$ vs blank control; ## means $p < 0.01$ vs blank control; * means $p < 0.05$ vs model group.

3.2. Exserolides decreased lipid accumulation in ox-LDL-laden RAW264.7 cells

Fig. 2A demonstrates that 50 mg/mL ox-LDL significantly increased lipid accumulation in RAW264.7 cells, as revealed by oil red O staining. In contrast, treatment with TO901317 or exserolides, particularly exserolide J, significantly decreased intracellular lipid accumulation. To more accurately quantify their lipid-lowering effects, intracellular TC and TG levels were measured using assay kits rather than the semiquantitative analysis of oil red O-stained areas. The LXR agonist TO901317 markedly decreased intracellular TC levels by 43.7 % ($P < 0.001$, Fig. 2B); however, it did not affect TG levels (Fig. 2C). Compounds I and J significantly decreased TC levels by 18.8 % ($P < 0.05$) and 35.6 % ($P < 0.01$), respectively. However, compounds E or F did not affect TC levels in ox-LDL-laden RAW264.7 cells (Fig. 2B). Moreover, exserolides, particularly compound J, significantly decreased intracellular TG levels (Fig. 2C). Therefore, although exserolides exhibited weaker TC-lowering effects, they exhibited better TG-lowering effects in RAW264.7 cells compared with TO901317.

To imitate the actual situation *in vivo*, plasma, rather than apolipoprotein A1 or HDL particle, was used as the acceptor in the following isotope tracing experiments. We observed that TO901317 significantly improved [³H]-cholesterol efflux by 94.7 % compared with the blank control ($P < 0.001$, Fig. 2D). Furthermore, compounds I and J enhanced [³H]-cholesterol efflux by 21.5 % and 38.8 %, respectively ($P < 0.05$, Fig. 2D). However, compounds E and F exhibited no significant effects on [³H]-cholesterol efflux, whereas compound E exhibited much weaker effects than compound J ($P < 0.05$, Fig. 2D).

3.3. Exserolide J enhanced ABCA1, LXR α , and PPAR α protein levels in ox-LDL- laden RAW264.7 cells

Many important membrane transporters, including ABCA1, ABCG1, and SR-B1, mediate cholesterol homeostasis in cells [6,16]. In our study, ox-LDL accumulation significantly decreased ABCA1 protein levels and increased ABCG1 protein levels compared with the blank control ($P < 0.05$, Fig. 3A and B). Furthermore, compared with the model group, TO901317 significantly increased ABCA1 and LXR α protein levels by approximately 15.9-fold ($P < 0.01$) and 61.7 % ($P < 0.05$), respectively (Fig. 3A and D); however, it did not affect ABCG1 protein levels (Fig. 3C). Importantly, exserolides I, J, E, and F significantly improved ABCA1 protein levels by 4.4-, 6.6-, 2.4-, and 4.9-fold, respectively, compared with the model group ($P < 0.05$, Fig. 3A). Notably, among these four exserolides, compound

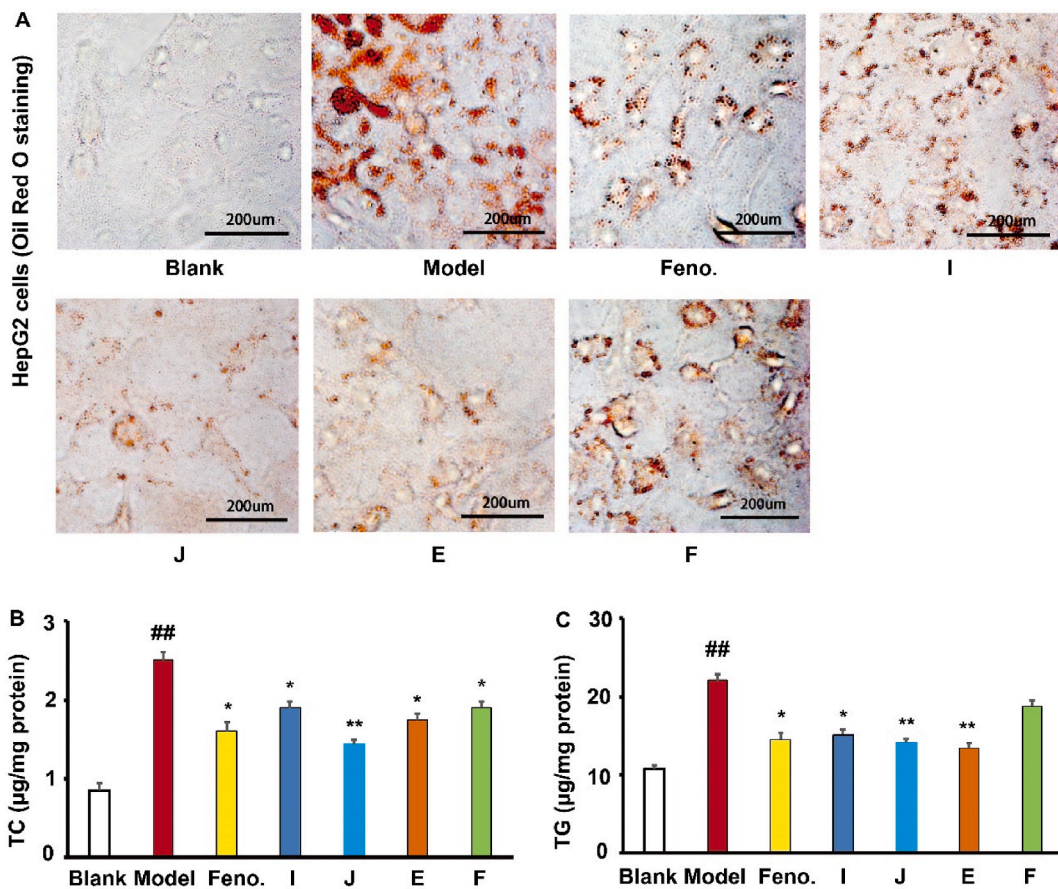


Fig. 4. Effects of exserolides on lipid accumulation in oleic acid-laden HepG2 cells (n = 3). A, typical pictures of oil red O staining; B, intracellular TC levels; C, intracellular TG levels. Feno.: fenofibrate.

J exhibited the highest effect on improving ABCA1 protein levels. Similar to 901317, these compounds did not affect ABCG1 protein levels compared with the model group. Moreover, ox-LDL accumulation significantly enhanced SR-B1 protein levels by 61.7 % ($P < 0.05$, Fig. 3C). The LXR α agonist significantly decreased SR-B1 expression by 57.5 % ($P < 0.01$). Interestingly, the four exselerolides, particularly compounds J and F, dramatically decreased SR-B1 protein levels (Fig. 3C); this suggests that these compounds inhibit lipid accumulation by suppressing SR-B1-mediated lipid uptake. Additional investigations indicated that compound J, but not compounds I, E, or F, significantly increased LXR α protein levels by 83.2 % ($P < 0.05$, Fig. 3D). Among the four exselerolides, only compound J significantly enhanced PPAR α protein levels by approximately 77.8 % ($P < 0.05$, Fig. 3E) in ox-LDL-laden RAW264.7 cells. Compared with the blank control, ox-LDL intervention significantly increased CD36 protein levels ($P < 0.05$, Fig. 3F). In addition, exselerolides J and E dramatically decreased CD36 protein levels by 67.2 % and 63.3 %, respectively ($P < 0.05$, Fig. 3F).

3.4. Exselerolides decreased lipid levels in oleic acid-laden HepG2 cells

Fig. 4A illustrates that 0.5 mM oleic acid treatment significantly increased lipid accumulation in HepG2 hepatocytes, whereas 2 μ M fenofibrate markedly decreased lipid levels in HepG2 cells, as revealed by oil red O staining. Notably, exselerolides significantly decreased intracellular accumulation. Further quantification using assay kits revealed that fenofibrate significantly decreased TC and TG levels by 43.2 % ($P < 0.01$, Figs. 4B) and 34.1 % ($P < 0.05$, Fig. 4C), respectively, compared with the model group. Furthermore, compounds I, J, E, and F markedly decreased intracellular TC levels by approximately 28.6 % ($P < 0.05$), 42.8 % ($P < 0.01$), 30.6 % ($P < 0.05$), and 28.3 % ($P < 0.05$), respectively, compared with the model group. Additionally, exselerolides I, J, E, and F significantly decreased TG levels by 31.4 % ($P < 0.05$), 35.9 % ($P < 0.01$), 38.9 % ($P < 0.01$), and 14.8 %, respectively, compared with the model group (Fig. 4C). Therefore, exselerolide J exhibited the best TC-lowering effect and exselerolide J was the most effective in TG-lowering in this study using lipid-laden HepG2 cells.

3.5. Exselerolides did not affect SR-B1, SREBP-2, LDLR, or PCSK9 protein levels in HepG2 cells

Fenofibrate did not affect SR-B1, LDLR, PCSK9, or SREBP-2 protein levels in HepG2 hepatocytes (Fig. 5). Fig. 5A illustrates that compound F decreased SR-B1 protein levels; however, this alteration did not exhibit significant differences, as revealed by three independent experiments. Similar to fenofibrate, the four exselerolides did not affect LDLR, PCSK9, or SREBP-2 protein levels compared with the vehicle group (Fig. 5B–D).

3.6. Exselerolide J increased PPAR α , CYP7A1, and LXR α protein levels in HepG2 cells

At the concentration of 2 μ M, fenofibrate, a PPAR α agonist, significantly improved PPAR α protein levels by approximately 44.0 % ($P < 0.05$, Fig. 6A). More importantly, exselerolides I, J, and E significantly improved PPAR α protein levels by 85.6 %, 56.4 %, and 60.7 %, respectively ($P < 0.05$, Fig. 6A). However, exselerolide F did not affect PPAR α levels. Furthermore, these four exselerolides exhibited no

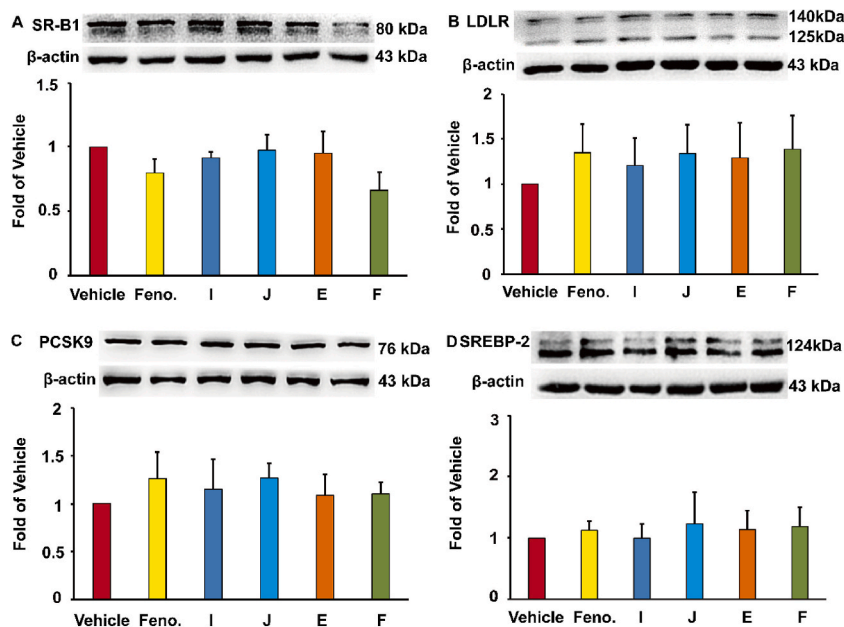


Fig. 5. Effects of exselerolides on SR-B1 (A), LDLR (B), precursor PCSK9 (C), and SREBP-2 (D) protein levels ($n = 3$). The raw images were provided as supplementary material for Fig. 5A–D.

effects on SREBP-1c protein levels as that of fenofibrate (Fig. 6B). CYP7A1 is a vital enzyme for converting cholesterol into bile acids. In our study, fenofibrate significantly enhanced CYP7A1 protein levels by approximately 87.1 % ($P < 0.05$, Fig. 6C). Interestingly, exersolide J, but not I, E, or F, significantly elevated CYP7A1 protein levels by approximately 51.4 % ($P < 0.05$, Fig. 6C), suggesting it enhances cholesterol conversion to bile acids. Furthermore, fenofibrate significantly enhanced LXR α levels by 64.5 % ($P < 0.05$, Fig. 6D). Interestingly, compound J, but not I, E, or F, dramatically elevated LXR α protein levels by 1.2-fold ($P < 0.05$, Fig. 6D). However, neither fenofibrate nor these four exersolides exhibited significant effects on ABCG8 protein levels (Fig. 6E).

3.7. Molecular docking between exersolides and LXR α or PPAR α protein

Fig. 7A illustrates that the docking score between LXR α protein and exersolide I was -7.7 kcal/mol (RMSD = 0.90 Å), suggesting an effective interaction between these two molecules. The hydroxyl group and several oxygen atoms of exersolide I could form hydrogen bonds with the hydrogen atoms of ILE336, PHE340, and HIS421 of LXR α . Hydrophobic interactions were observed between exersolide I and THR302, PHE326, LEU331, and ILE339 of LXR α protein. Furthermore, PHE335 of LXR α protein and exersolide I could form π -stacking (perpendicular). Notably, among the four compounds, exersolide J exhibited the strongest interaction with LXR α protein, with a docking score of -7.9 kcal/mol (RMSD = 1.94 Å) (Fig. 7B). ALA261, SER264, and THR302 of LXR α protein could form hydrogen bonds with exersolide J, whereas PHE257, LEU260, and TRP443 formed hydrophobic interactions with exersolide J. Importantly, PHE335 of LXR α protein and exersolide J could form π -stacking in a parallel model, whereas the amino acid HIS421 of LXR α protein formed a salt bridge with the carboxyl group of exersolide J; this contributed to the strong interaction between LXR α protein and exersolide J (Fig. 7B). Fig. 7C illustrates that among the four exersolides, exersolide E exhibited the weakest interaction with LXR α protein (docking score: -6.5 kcal/mol, RMSD = 1.12 Å). This compound formed weak hydrogen bonds with THR302 of LXR α protein. Furthermore, the amino acids PHE254, THR258, ALA261, LEU331, PHE335, and LEU428 of LXR α formed hydrophobic interactions with exersolide E. Moreover, the docking score between exersolide F and LXR α protein was -7.7 kcal/mol (RMSD = 0.99 Å) (Fig. 7D). SER264 and THR302 of LXR α could form hydrogen bonds with compound F, whereas PHE257, THR258, and LEU 260

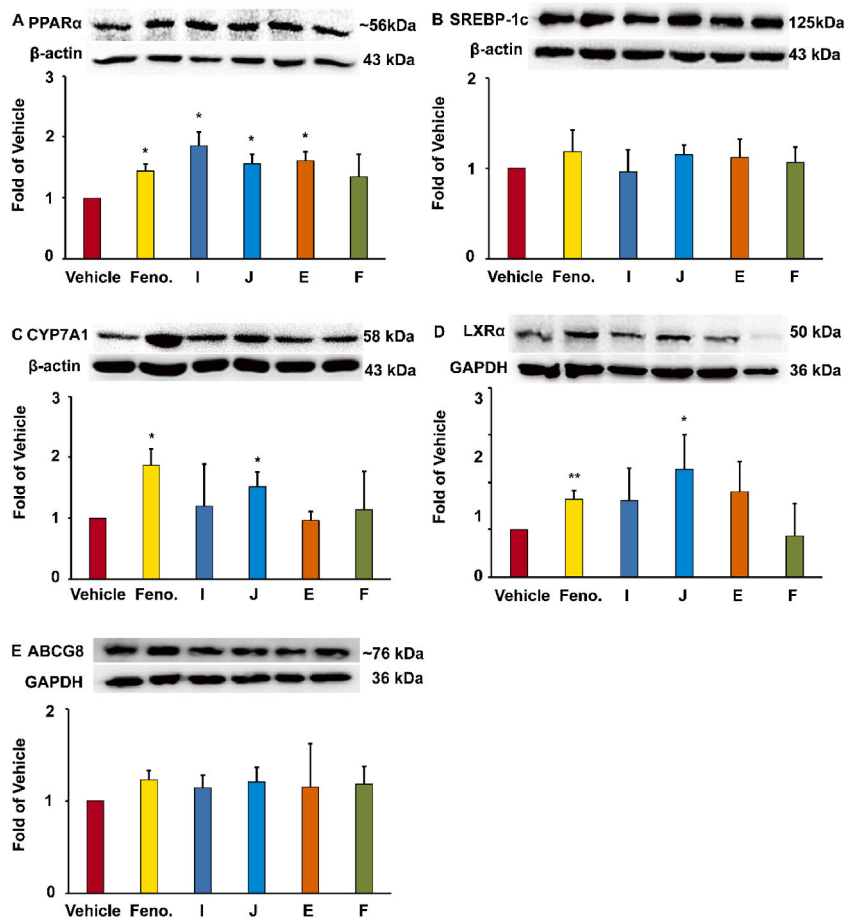


Fig. 6. Effects of exersolides on PPAR α (A, $n = 3$), SREBP-1c (B, $n = 3$), CYP7A1 (C, $n = 3$), LXR α (D, $n = 4$), and ABCG8 (E, $n = 3$) protein levels in HepG2 hepatocytes. The raw images were provided as supplementary material for Fig. 6A–E. * means $p < 0.05$ vs vehicle group; ** means $p < 0.01$ vs vehicle group.

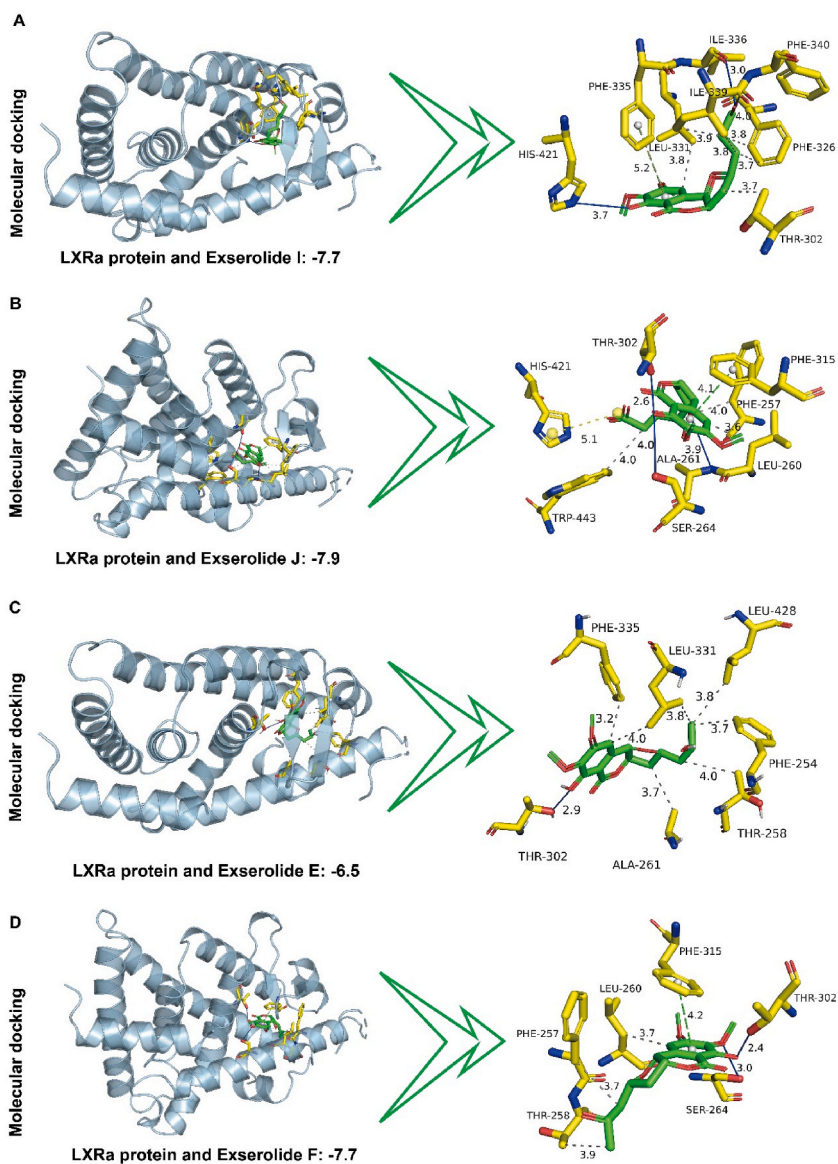


Fig. 7. Interactions between exserolides and LXR α protein, as reveal by molecule docking. A, the interaction between exserolide I and LXR α protein; B, the interaction between exserolide J and LXR α protein; C, the interaction between exserolide E and LXR α protein; D, the interaction between exserolide F and LXR α protein.

formed hydrophobic interactions with this compound. Additionally, π -stacking (parallel) was observed between PHE315 of LXR α protein and compound F.

Fig. 8 summarized the molecule docking data between exserolides and PPAR α protein. Exserolide I interacted with the amino acid TYR334 via hydrogen bonds. Furthermore, it formed hydrophobic interactions with THR279 and MET320 of PPAR α protein. The docking score was -7.6 kcal/mol (RMSD = 0.76 Å) (Fig. 8A). Exserolide J had a higher docking score (-8.0 kcal/mol, RMSD = 1.15 Å) compared with exserolide I, suggesting a stronger interaction. Fig. 8B illustrates that ASN219, MET220, THR279, GLU286, ALA333, and TYR334 of PPAR α protein formed hydrogen bonds, whereas THR279, LEU321, and VAL324 of PPAR α protein formed hydrophobic interactions with exserolide J. Interestingly, the interaction between exserolide E and PPAR α (docking score: -8.1 kcal/mol, RMSD = 0.74 Å, Fig. 8C) was similar to that between exserolide J and PPAR α . THR279, THR283, ALA333, and TYR334 of PPAR α protein could form hydrogen bonds, whereas PHE218, MET220, THR279, THR283, and LEU321 formed hydrophobic interactions with exserolide E. Additionally, exserolide F could interact with THR283, TYR334, and GLY335 of PPAR α protein via hydrogen bonds, and formed hydrophobic interactions with MET220, THR279, THR283, ILE317, MET320, and LEU321 of PPAR α protein. The docking score between exserolide F and PPAR α protein was -7.8 kcal/mol (RMSD = 1.12 Å) (Fig. 8D).

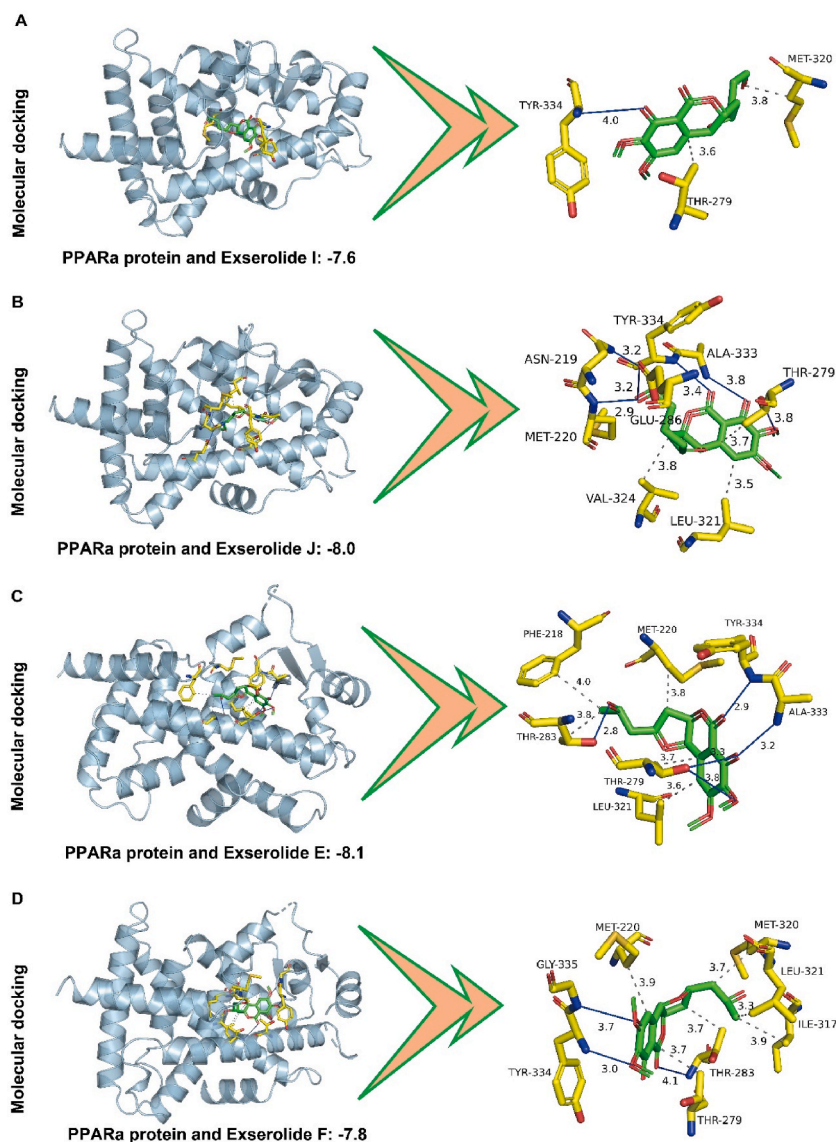


Fig. 8. Interactions between exserolides and PPAR α protein, as reveal by molecule docking. A, the interaction between exserolide I and PPAR α protein; B, the interaction between exserolide J and PPAR α protein; C, the interaction between exserolide E and PPAR α protein; D, the interaction between exserolide F and PPAR α protein.

4. Discussion

Given the vital roles of peripheral cells, such as macrophages, and hepatic cells in the process of RCT as described in the introduction section, two cell lines were used to establish lipid-laden models in the present study. Briefly, RAW264.7 cells and HepG2 cells were used to imitate peripheral cells and hepatic cells, respectively. In this study, we observed that four exserolides, particularly exserolide J, can decrease ox-LDL-laden lipid accumulation and cholesterol efflux primarily by activating the LXR α –ABCA1 signaling pathway and PPAR α expression and decreasing CD36-mediated lipid uptake in RAW264.7 macrophages. Furthermore, these four exserolides can decrease intracellular TC and TG levels in lipid-laden HepG2 cells. In addition, exserolides I, J, and E can enhance PPAR α protein levels. Notably, compound J significantly improved CYP7A1 and LXR α protein levels in HepG2 cells. Molecule docking revealed that exserolide J exhibits the strongest interaction with LXR α and exserolide J and E exhibit powerful interaction with PPAR α protein. However, exserolide E exhibits the weakest interaction with LXR α protein. Collectively, these data suggest that the terminal carboxyl group of exserolide J contributes to its lipid-lowering effects by interacting with LXR α and PPAR α proteins.

Hyperlipidemia, characterized by abnormally increased non-HDL-c and TG levels, contributes to the onset and development of atherosclerosis and other lipid metabolism-associated diseases [1–6]. RCT is a physiological process in which excess peripheral cholesterol is transported to the liver for conversion and/or excretion. Studies suggest that RCT can attenuate hyperlipidemia [6,11,

16]. In this study, the positive control TO901317 exerted powerful effects on improving ABCA1 and LXR α levels. These data were consistent with those of previous studies [27,28]. Importantly, we observed that exselerolides not only decreased ox-LDL-laden lipid accumulation but also enhanced [^3H]-cholesterol efflux from RAW264.7 macrophages. It is worth noting that exselerolides I and J exhibited better TC-lowering and cholesterol efflux-improving effects than exselerolides E and F, suggesting the terminal carboxyl or hydroxyl group benefits the TC-lowering effects of exselerolides. ABCA1 mediates cholesterol efflux to apolipoprotein A1, and ABCG1 mediates cholesterol efflux to HDL particles [5,6,28]. In line with the TC-lowering effects, these exselerolides, particularly compound J, significantly improved ABCA1 protein levels, suggesting that the terminal carboxyl group of compound J contributes to ABCA1 improving effects of exselerolides. Moreover, SR-B1 plays a key role in cholesterol homeostasis in macrophages. The four exselerolides significantly decreased SR-B1 protein levels as that of TO901317. Therefore, exselerolides may improve RCT by enhancing ABCA1 protein levels and inhibiting SR-B1 protein. LXR α is an activator of ABC transporters [16,33]. In the present study, exselerolide J significantly enhanced LXR α protein levels as that of the LXR α agonist TO901317, suggesting that this compound enhances the LXR α /ABCA1 signaling pathway. However, the increased multiple of ABCA1 protein was much greater than that of ABCG1 or LXR α protein, suggesting that ABCA1 expression was more sensitive after LXR α activation. Furthermore, exselerolide J exhibited the strongest effect on improving the levels of PPAR α , a key protein responsible for TG hydrolysis via fatty acid β -oxidation. Interestingly, PPAR α activation can induce ABC transporter expression; therefore, exselerolide J may also improve the first step of RCT in macrophages by upregulating PPAR α expression [12,34,35]. In addition, the terminal carboxyl group of exselerolide J may decrease the levels of CD36 protein, a typical class B scavenger receptor responsible for the uptake of modified lipoproteins, including ox-LDL, in macrophages [36].

Ligand–protein interactions are used to investigate mechanisms of action of bioactive compounds, and PLIP is a useful tool in this field [25]. Interestingly, exselerolide J exhibited the strongest interaction with LXR α protein, followed by exselerolides I, F, and E. Notably, the ligand-binding sites of TO901317 with LXR α are demonstrated to include THR302, TRP443, HIS421, and PHE257 [37, 38], which are consistent with the binding sites between exselerolides and LXR α protein in this study. Furthermore, the docking score between exselerolide J and LXR α (-7.9 kcal/mol) was close to that of TO901317 and LXR α (-10.8 and -7.5695 kcal/mol), as demonstrated by distinct groups [38,39]. Importantly, the RMSD values were less than 2.0 Å, suggesting the accuracy of the docking method in our study [31,32]. Additionally, the carboxylic group is demonstrated to contribute the formation of hydrogen bonds with THR302, HIS421, and TRP443, and the basic phenyl structure may contribute to the formation of π -stacking with amino acids, such as PHE [37,40,41]. These molecular docking data were consistent with ABCA1 and LXR α protein levels after treating RAW264.7 macrophages with exselerolides (Fig. 3). Among the exselerolides, exselerolide J exhibited the best effects on ABCA1, a downstream molecule of LXR α . Furthermore, compound J exhibited a powerful effect on LXR α protein stimulation in HepG2 cells. Therefore, our molecular docking data further confirm that exselerolide J may directly activate the LXR α /ABC transporter pathway.

In this study, the positive control fenofibrate significantly decreased intracellular TC and TG levels in HepG2 cells. This finding is consistent with that of previous studies [28,42]. Importantly, the four exselerolides, particularly compounds J and E, exhibited powerful effects on decreasing oleic acid-induced TC and TG accumulation in HepG2 cells compared with the model group. LDLR and SR-B1 mediate the transfer of non-HDL-c and HDL-c, respectively, to hepatic cells for metabolism [4–6]. PCSK9 binds to the epidermal growth factor-like repeat A domain of LDLR, inducing its degradation [43]. However, these four exselerolides did not significantly affect LDLR and PCSK9 proteins, suggesting that they do not affect lipoprotein uptake via LDLR. SREBPs are important transcription factors involved in regulating lipid metabolism and homeostasis in the liver. The SREBP family comprises three members: SREBP-1a, SREBP-1c, and SREBP-2 [44]. SREBP-2 is tightly regulated by the cholesterol content in the endoplasmic reticulum; it specifically modulates the genes involved in cholesterol synthesis and uptake, including HMG-CoA reductase, PCSK9, and LDLR, thereby modulating cholesterol homeostasis [44]. However, in our study, the four exselerolides did not affect SREBP-2 protein levels as that of fenofibrate. Among the four exselerolides, no compound significantly affected SR-B1 levels, suggesting these compounds do not affect the SR-B1-mediated transfer of HDL particles. These insignificant data in Fig. 5 may be partially induced by the lipid-laden model used in the present study. Given cells were pre-loaded with sufficient lipids before the addition of exselerolides, the lipid uptake-related molecules including SR-B1, LDLR, and PCSK9, and lipid synthesis-related proteins, such as SREBP-2 and SREBP-1c, may be suppressed as a feedback mechanism or even lose efficacy. Therefore, it is hard to observe obvious differences among groups. However, this model may activate lipid catabolism and excretion mechanisms as discussed in the following.

CYP7A1, a downstream molecule of LXR α , converts cholesterol to 7- α -hydroxycholesterol, which is the first and rate-limiting step in bile acid synthesis, thereby contributing to cholesterol metabolism [13]. Interestingly, exselerolide J may accelerate the conversion of cholesterol to bile acid by enhancing CYP7A1 protein levels. However, the other three exselerolides did not significantly affect CYP7A1 protein levels. These results indicate that the substitution of $-\text{COOH}$ at C12 (CH_2COOH) of exselerolide benefits CYP7A1 expression by activating LXR α . These data are consistent with the strongest interaction between exselerolide J and LXR α protein (Fig. 7). Studies have revealed that ABCG5 and ABCG8 play key roles in biliary sterol secretion and RCT [14,15]. However, the four exselerolides may not affect ABCG8-mediated lipid excretion.

SREBP-1c regulates the expression of lipogenic genes, including acetyl-CoA carboxylase and fatty acid synthase, thereby regulating the synthesis of fatty acid and TG [4,44]. In this study, we observed that the four exselerolides did not affect SREBP-1c protein levels, suggesting that these compounds do not affect TG synthesis. However, investigating whether these compounds induce lipogenesis *in vivo* in the future is vital. PPAR α is a nuclear hormone receptor that is activated by fatty acids and their derivatives; it is the primary target of fibrates, a class of widely used drugs [12,45]. In line with the findings of a previous review [12], the PPAR α agonist fenofibrate significantly improved PPAR α protein levels in HepG2 cells. Interestingly, exselerolides, particularly compounds J and E significantly improved PPAR α protein levels, and the effects were even higher than those of fenofibrate; this indicates the terminal carboxyl group and the configuration of the hydroxyl group play a key role in regulating of PPAR α expression. Importantly, our

molecule docking data confirmed that exeserolides J and E form stronger interactions with PPAR α protein compared with exeserolides I and F. In line with our finding, previous studies demonstrate that PPAR α ligands may bind with the amino acids including TYR334, THR279, LEU321, ALA333, and MET220 [26,30,46]. The docking scores between exeserolides and PPAR α (ranging from -7.6 to -8.1 kcal/mol) were close to that of fenofibrate and PPAR α (-6.24 or -11.525 kcal/mol), as revealed by distinct groups [26,47]. Moreover, the RMSD values between exeserolides and PPAR α were less than 2.0 \AA , indicating the accuracy of the docking process and credible of these data [31,32]. Our data demonstrated that exeserolides J and E may directly activate PPAR α . It is worth noting that compounds I and E exhibited different effects on PPAR α protein levels in distinct cell models, suggesting that cellular environments and cell type modulate the final effects of these molecules. Although compounds I, E, and F exhibited no significant effects on PPAR α and LXR α protein levels, these molecules also demonstrated hypolipidemic effects in RAW264.7 cells by improving ABCA1 protein levels, indicating that the basic exeserolide structure exerts lipid-lowering effects via some unknown mechanisms of action, which should be further investigated. Indeed, this may also be explained by the distinct sensitivity of these proteins, including LXR α and ABCA1, after exeserolide intervention, as discussed above.

In conclusion, four exeserolides, particularly compound J, exhibited good lipid-lowering capacity. Their underlying mechanisms of action are similar to but not limited to that of fenofibrate or the LXR α agonist TO901317. Interestingly, exeserolide J accelerates the first step of RCT by stimulating ABCA1; furthermore, it may enhance bile acid production by improving CYP7A1 protein levels. The mechanisms of action of exeserolide J on activating ABCA1 and CYP7A1 may be attributed to its interactions with LXR α and PPAR α , as demonstrated by molecule docking and western blotting. Importantly, the terminal carboxyl group of exeserolide J contributes to its hypolipidemic effects *in vitro*. Considering that TO901317 induces severe lipogenesis [48] and exeserolide J exhibits no significant effects on SREBP-1c *in vitro*, this molecule may be explored as a potential compound for preventing or treating lipid disorders. Presumably, the appropriate activation of LXR α and not the intensive activation of LXR α , similar to 901317, is important for maintaining lipid homeostasis and avoiding side effects such as lipogenesis.

However, there are some limitations in the present study. It is estimated that approximately 50 % of drug research and development failures are originated from the *in vivo* pharmacokinetic properties, particularly hepatic metabolism, of the interested compound [49]. Cytochrome P450 (CYP) enzymes and other enzymes, such as UDP-glucuronosyltransferases, play vital roles in the metabolism of xenobiotics. Several literatures have demonstrated that isocoumarins may interact with CYP family members, such as CYP2D6 [49,50]. Based on these available literatures, exeserolides, a minor existing form of isocoumarin, are predicted to be metabolized into their hydroxy and/or ester forms as well as conjugated derivatives with glutathione, sulfate, and glucuronic acid groups. However, these predictions need to be investigated using the modern analysis techniques, such as liquid chromatography-tandem mass spectrometry, in the future [50,51]. Considering the potential cytotoxicity, whether these exeserolides exhibit similar lipid-lowering effects at concentrations of less than $5.0 \mu\text{M}$ need to be investigated in the future. Given these exeserolides exhibit insignificant effects on hepatic proteins that are related to lipoprotein absorption, whether these exeserolides exert their lipid-regulatory effects in normal hepatic cells via modulating these proteins also need to be clarified in the future. As exeserolide J is demonstrated to lower intracellular levels of TC via activating LXR α , the *in vivo* lipid-lowering effects of this compound, particularly its effects on lipogenesis, should to be clarified in the future.

Funding

This work was supported by National Natural Science Foundation of China (82070469, 82271803).

Data availability statement

Data are available from the corresponding author upon reasonable request.

Ethical approval

Ethical approval is not applicable to this study.

CRediT authorship contribution statement

Yan Zhang: Writing – original draft, Investigation, Formal analysis. **Xue Wang:** Investigation, Data curation. **Tian Liu:** Investigation, Formal analysis, Data curation. **Zi-Yi Zhang:** Software, Resources, Investigation. **Wen-Gang Song:** Writing – review & editing, Supervision, Project administration, Funding acquisition. **Shou-Dong Guo:** Writing – review & editing, Supervision.

Declaration of competing interest

The authors declare the following financial interests/personal relationships which may be considered as potential competing interests: Wen-gang Song reports financial support was provided by National Natural Science Foundation of China. Shou-dong Guo reports financial support was provided by National Natural Science Foundation of China. Not applicable. reports a relationship with Not applicable. that includes: Not applicable. has patent Not applicable. pending to Not applicable. Not applicable. If there are other authors, they declare that they have no known competing financial interests or personal relationships that could have appeared to influence the work reported in this paper.

Acknowledgement

We thank professor Jun-Feng Wang and Hong Liu at South China Sea Institute of Oceanology (Chinese Academy of Sciences) for providing these four exselerolides.

Appendix A. Supplementary data

Supplementary data to this article can be found online at <https://doi.org/10.1016/j.heliyon.2024.e31861>.

References

- [1] A. Pirillo, M. Casula, E. Olmastroni, G.D. Norata, A.L. Catapano, Global epidemiology of dyslipidaemias, *Nat. Rev. Cardiol.* 18 (10) (2021) 689–700, <https://doi.org/10.1038/s41569-021-00541-4>.
- [2] S. Sharma, K. Gaur, R. Gupta, Trends in epidemiology of dyslipidemias in India, *Indian Heart J.* 76 (Suppl 1) (2024) S20–S28, <https://doi.org/10.1016/j.ihj.2023.11.266>, Suppl 1.
- [3] M. Mutalifu, Q. Zhao, Y. Wang, X. Hamulati, Y.S. Wang, L. Deng, N. Adili, F. Liu, Y.N. Yang, X.M. Li, Joint association of physical activity and diet quality with dyslipidemia: a cross-sectional study in Western China, *Lipids Health Dis.* 23 (1) (2024) 46, <https://doi.org/10.1186/s12944-024-02030-2>.
- [4] B.H. Zhang, F. Yin, Y.N. Qiao, S.D. Guo, Triglyceride and triglyceride-rich lipoproteins in atherosclerosis, *Front. Mol. Biosci.* 9 (2022) 909151, <https://doi.org/10.3389/fmolb.2022.909151>.
- [5] J.L.M. Björkegren, A.J. Lusis, Atherosclerosis: recent developments, *Cell* 185 (10) (2022) 1630–1645, <https://doi.org/10.1016/j.cell.2022.04.004>.
- [6] H. Li, X.H. Yu, X. Ou, X.P. Ouyang, C.K. Tang, Hepatic cholesterol transport and its role in non-alcoholic fatty liver disease and atherosclerosis, *Prog. Lipid Res.* 83 (2021) 101109, <https://doi.org/10.1016/j.plipres.2021.101109>.
- [7] S. Attardo, O. Musumeci, D. Velardo, A. Toscano, Statins neuromuscular adverse effects, *Int. J. Mol. Sci.* 23 (15) (2022) 8364, <https://doi.org/10.3390/ijms23158364>.
- [8] A. Gupta, D. Thompson, A. Whitehouse, T. Collier, B. Dahlof, N. Poulter, R. Collins, P. Sever, ASCOT Investigators, Adverse events associated with unblinded, but not with blinded, statin therapy in the Anglo-Scandinavian Cardiac Outcomes Trial-Lipid-Lowering Arm (ASCOT-LLA): a randomised double-blind placebo-controlled trial and its non-randomised non-blind extension phase, *Lancet* 389 (10088) (2017) 2473–2481, [https://doi.org/10.1016/S0140-6736\(17\)31075-9](https://doi.org/10.1016/S0140-6736(17)31075-9).
- [9] E. Gallego-Colon, A. Daum, C. Yosefy, Statins and PCSK9 inhibitors: a new lipid-lowering therapy, *Eur. J. Pharmacol.* 878 (2020) 173114, <https://doi.org/10.1016/j.ejphar.2020.173114>.
- [10] Y. Chen, S. Yang, L. Liu, X. Yang, Y. Duan, S. Zhang, J. Han, A novel therapy for hepatic cholestasis treatment—the combination of rosiglitazone and fenofibrate, *Eur. J. Pharmacol.* 938 (2023) 175428, <https://doi.org/10.1016/j.ejphar.2022.175428>.
- [11] S. Sacher, A. Mukherjee, A. Ray, Deciphering structural aspects of reverse cholesterol transport: mapping the knowns and unknowns, *Biol. Rev. Camb. Phil. Soc.* 98 (4) (2023) 1160–1183, <https://doi.org/10.1111/brv.12948>.
- [12] M. Miao, X. Wang, T. Liu, Y.J. Li, W.Q. Yu, T.M. Yang, S.D. Guo, Targeting PPARs for therapy of atherosclerosis: a review, *Int. J. Biol. Macromol.* 242 (Pt 2) (2023) 125008, <https://doi.org/10.1016/j.ijbiomac.2023.125008>.
- [13] K.R. Feingold, Lipid and lipoprotein metabolism, *Endocrinol Metab. Clin. N. Am.* 51 (3) (2022) 437–458, <https://doi.org/10.1016/j.ecl.2022.02.008>.
- [14] A.B. Singh, B. Dong, F.B. Kraemer, J. Liu, FXR activation promotes intestinal cholesterol excretion and attenuates hyperlipidemia in SR-B1-deficient mice fed a high-fat and high-cholesterol diet, *Phys. Rep.* 8 (5) (2020) e14387, <https://doi.org/10.14814/phy2.14387>.
- [15] H. Hu, W. Shao, Q. Liu, N. Liu, Q. Wang, J. Xu, X. Zhang, Z. Weng, Q. Lu, L. Jiao, C. Chen, H. Sun, Z. Jiang, X. Zhang, A. Gu, Gut microbiota promotes cholesterol gallstone formation by modulating bile acid composition and biliary cholesterol secretion, *Nat. Commun.* 13 (1) (2022) 252, <https://doi.org/10.1038/s41467-021-27758-8>.
- [16] X.H. Yu, D.W. Zhang, X.L. Zheng, C.K. Tang, Cholesterol transport system: an integrated cholesterol transport model involved in atherosclerosis, *Prog. Lipid Res.* 73 (2018) 65–91, <https://doi.org/10.1016/j.plipres.2018.12.002>.
- [17] S. Xiao, N. Chen, Z. Chai, M. Zhou, C. Xiao, S. Zhao, X. Yang, Secondary Metabolites from Marine-Derived *Bacillus*: a comprehensive review of origins, structures, and bioactivities, *Mar. Drugs* 20 (9) (2022) 567, <https://doi.org/10.3390/md20090567>.
- [18] J.D.M. de Sá, D. Kumla, T. Dethoup, A. Kijjoo, Bioactive compounds from terrestrial and marine-derived fungi of the genus *Neosartorya*, *Molecules* 27 (7) (2022) 2351, <https://doi.org/10.3390/molecules27072351>.
- [19] M.A. Tammam, M.I. Gamal El-Din, A. Abood, A. El-Demerdash, Recent advances in the discovery, biosynthesis, and therapeutic potential of isocoumarins derived from fungi: a comprehensive update, *RSC Adv.* 13 (12) (2023) 8049–8089, <https://doi.org/10.1039/d2ra08245d>.
- [20] G. Shabir, A. Saeed, H.R. El-Seedi, Natural isocoumarins: structural styles and biological activities, the revelations carry on, *Phytochemistry* 181 (2021) 112568, <https://doi.org/10.1016/j.phytochem.2020.112568>.
- [21] D. Wang, V. Hiebl, T. Xu, A. Ladurner, A.G. Atanasov, E.H. Heiss, V.M. Dirsch, Impact of natural products on the cholesterol transporter ABCA1, *J. Ethnopharmacol.* 249 (2020) 112444, <https://doi.org/10.1016/j.jep.2019.112444>.
- [22] J.Y. Kim, S. Kim, S.H. Shim, Anti-Atherosclerotic activity of (3R)-5-hydroxymellein from an endophytic fungus *Neofusicoccum parvum* JS-0968 derived from *vitex rotundifolia* through the inhibition of lipoproteins oxidation and foam cell formation, *Biomolecules* 10 (5) (2020) 715, <https://doi.org/10.3390/biom10050715>.
- [23] X.Y. Pang, X.P. Lin, J. Yang, X. Zhou, B. Yang, J. Wang, Y. Liu, Spiro-phthalides and isocoumarins isolated from the marine-sponge-derived fungus *Setosphaeria* sp. SCSIO41009, *J. Nat. Prod.* 81 (8) (2018) 1860–1868, <https://doi.org/10.1021/acs.jnatprod.8b00345>.
- [24] X. Pang, B. Yang, X. Zhou, J. Wang, J. Yang, Y. Liu, Two new isocoumarins isolated from the marine-sponge-derived fungus *Setosphaeria* sp. SCSIO41009, *Chem. Biodivers.* 21 (4) (2024) e202302069, <https://doi.org/10.1002/cbdv.202302069>.
- [25] M.F. Adame, K.L. Linnemann, S.N. Bolz, F. Kaiser, S. Salentin, V. Joachim Haupt, M. Schroeder, Plip 2021: expanding the scope of the protein-ligand interaction profiler to DNA and RNA, *Nucleic Acids Res.* 49 (W1) (2021) W530–W534, <https://doi.org/10.1093/nar/gkab294>.
- [26] S. Ballav, K.B. Lokhande, R.S. Yadav, P. Ghosh, K.V. Swamy, S. Basu, Exploring binding mode assessment of novel kaempferol, resveratrol, and quercetin derivatives with PPAR- α as potential drug candidates against cancer, *Mol. Divers.* 27 (6) (2023) 2867–2885, <https://doi.org/10.1007/s11030-022-10587-2>.
- [27] T. Li, J.Y. Yin, Y.B. Ji, P. Lin, Y.J. Li, Z.X. Yang, S.M. Hu, J. Wang, B.H. Zhang, S. Koshti, J.F. Wang, C.F. Ji, S.D. Guo, Setosphayrone C and D accelerate macrophages cholesterol efflux by promoting LXR α /ABCA1 pathway, *Arch. Pharm. Res. (Seoul)* 43 (8) (2020) 788–797, <https://doi.org/10.1007/s12272-020-01255-w>.
- [28] T. Li, S.M. Hu, X.Y. Pang, J.F. Wang, J.Y. Yin, F.H. Li, J. Wang, X.Q. Yang, B. Xia, Y.H. Liu, W.G. Song, S.D. Guo, The marine-derived furanone reduces intracellular lipid accumulation *in vitro* by targeting LXR α and PPAR α , *J. Cell Mol. Med.* 24 (6) (2020) 3384–3398, <https://doi.org/10.1111/JCMM.15012>.
- [29] Y. Bian, X. Li, X. Li, J. Ju, H. Liang, X. Hu, L. Dong, N. Wang, J. Li, Y. Zhang, B. Yang, Daming capsule, a hypolipidaemic drug, lowers blood lipids by activating the AMPK signalling pathway, *Biomed. Pharmacother.* 117 (2019) 109176, <https://doi.org/10.1016/j.biopha.2019.109176>.
- [30] S. Mandal, S. Faizan, N.M. Raghavendra, B.R.P. Kumar, Molecular dynamics articulated multilevel virtual screening protocol to discover novel dual PPAR α / γ agonists for anti-diabetic and metabolic applications, *Mol. Divers.* 27 (6) (2023) 2605–2631, <https://doi.org/10.1007/s11030-022-10571-w>.

- [31] M. Zhang, X. Zhang, J. Pei, B. Guo, G. Zhang, M. Li, L. Huang, Identification of phytochemical compounds of *Fagopyrum dibotrys* and their targets by metabolomics, network pharmacology and molecular docking studies, *Heliyon* 9 (3) (2023) e14029, <https://doi.org/10.1016/j.heliyon.2023.e14029>.
- [32] Z. Nawaz, N. Riaz, M. Saleem, A. Iqbal, S. Abida Ejaz, B. Bashir, S. Muzaffar, M. Ashraf, Aziz Ur-Rehman, M. Sajjad Bilal, B. Krishna Prabhala, S. Sajid, Molecular hybrids of substituted phenylcarbamoylpiperidine and 1,2,4-triazole methylacetamide as potent 15-LOX inhibitors: design, synthesis, DFT calculations and molecular docking studies, *Bioorg. Chem.* 143 (2024) 106984, <https://doi.org/10.1016/j.bioorg.2023.106984>.
- [33] B. Wang, P. Tontonoz, Liver X receptors in lipid signalling and membrane homeostasis, *Nat. Rev. Endocrinol.* 14 (8) (2018) 452–463, <https://doi.org/10.1038/s41574-018-0037-x>.
- [34] R.A.K. Srivastava, A.B. Cefalu, N.S. Srivastava, M. Averna, NPC1L1 and ABCG5/8 induction explain synergistic fecal cholesterol excretion in ob/ob mice treated with PPAR- α and LXR agonists, *Mol. Cell. Biochem.* 473 (1–2) (2020) 247–262, <https://doi.org/10.1007/s11010-020-03826-3>.
- [35] V.R. More, C.R. Campos, R.A. Evans, K.D. Oliver, G.N. Chan, D.S. Miller, R.E. Cannon, PPAR- α , a lipid-sensing transcription factor, regulates blood-brain barrier efflux transporter expression, *J. Cerebr. Blood Flow Metabol.* 37 (4) (2017) 1199–1212, <https://doi.org/10.1177/0271678X16650216>.
- [36] L. Zhao, Z. Varghese, J.F. Moorhead, Y. Chen, X.Z. Ruan, CD36 and lipid metabolism in the evolution of atherosclerosis, *Br. Med. Bull.* 126 (1) (2018) 101–112, <https://doi.org/10.1093/bmb/ldy006>.
- [37] Y.N. Lin, C.C.N. Wang, H.Y. Chang, F.Y. Chu, Y.A. Hsu, W.K. Cheng, W.C. Ma, C.J. Chen, L. Wan, Y.P. Lim, Ursolic acid, a novel liver X receptor α (LXR α) antagonist inhibiting ligand-induced nonalcoholic fatty liver and drug-induced lipogenesis, *J. Agric. Food Chem.* 66 (44) (2018) 11647–11662, <https://doi.org/10.1021/acs.jafc.8b04116>.
- [38] S. Bedi, G.V. Hines, V.V. Lozada-Fernandez, C. de Jesus Piva, A. Kaliappan, S.D. Jr Rider, H.A. Hostetler, Fatty acid binding profile of the liver X receptor α , *J. Lipid Res.* 58 (2) (2017) 393–402, <https://doi.org/10.1194/jlr.M072447>.
- [39] W.Y. Gao, P.Y. Chen, H.J. Hsu, J.W. Liou, C.L. Wu, M.J. Wu, J.H. Yen, Xanthohumol, a prenylated chalcone, regulates lipid metabolism by modulating the LXR α /RXR-ANGPTL3-LPL axis in hepatic cell lines and high-fat diet-fed zebrafish models, *Biomed. Pharmacother.* 174 (2024) 116598, <https://doi.org/10.1016/j.biopha.2024.116598>.
- [40] Z. Liang, T. Gu, J. Wang, J. She, Y. Ye, W. Cao, X. Luo, J. Xiao, Y. Liu, L. Tang, X. Zhou, Chromene and chromone derivatives as liver X receptors modulators from a marine-derived *Pestalotiopsis neglecta* fungus, *Bioorg. Chem.* 112 (2021) 104927, <https://doi.org/10.1016/j.bioorg.2021.104927>.
- [41] Y. Fang, J. She, X. Zhang, T. Gu, D. Xie, X. Luo, X. Yi, C. Gao, Y. Liu, C. Zhang, L. Tang, X. Zhou, Discovery of anti-hypercholesterolemia agents targeting LXR α from marine microorganism-derived natural products, *J. Nat. Prod.* 87 (2) (2024) 322–331, <https://doi.org/10.1021/acs.jnatprod.3c01029>.
- [42] J. Yoo, I.K. Jeong, K.J. Ahn, H.Y. Chung, Y.C. Hwang, Fenofibrate, a PPAR α agonist, reduces hepatic fat accumulation through the upregulation of TFEB-mediated lipophagy, *Metabolism* 120 (2021) 154798, <https://doi.org/10.1016/j.metabol.2021.154798>.
- [43] K. Németh, B. Tóth, F. Sarnyai, A. Koncz, D. Lenzinger, É. Kereszturi, T. Visnovitz, B.M. Kestecher, X. Osteikoetxea, M. Csala, E.I. Buzás, V. Tamási, High fat diet and PCSK9 knockout modulates lipid profile of the liver and changes the expression of lipid homeostasis related genes, *Nutr. Metab.* 20 (1) (2023) 19, <https://doi.org/10.1186/s12986-023-00738-z>.
- [44] R.A. DeBose-Boyd, J. Ye, SREBPs in lipid metabolism, insulin signaling, and beyond, *Trends Biochem. Sci.* 43 (5) (2018) 358–368, <https://doi.org/10.1016/j.tibs.2018.01.005>.
- [45] S. Kersten, R. Stienstra, The role and regulation of the peroxisome proliferator activated receptor alpha in human liver, *Biochimie* 136 (2017) 75–84, <https://doi.org/10.1016/j.biochi.2016.12.019>.
- [46] A. Sandoval-Rodríguez, H.C. Monroy-Ramírez, A. Meza-Ríos, J. García-Bañuelos, J. Vera-Cruz, J. Gutiérrez-Cuevas, J. Silva-Gómez, B. Staels, J. Domínguez-Rosales, M. Galicia-Moreno, M. Vázquez-Del Mercado, J. Navarro-Partida, A. Santos-García, J. Armendariz-Borunda, Pirfenidone is an agonistic ligand for PPAR α and improves NASH by activation of SIRT1/LKB1/pAMPK, *Hepatol. Commun.* 4 (3) (2020) 434–449, <https://doi.org/10.1002/hep4.1474>.
- [47] F.U. Hassan, M.S. Rehman, M. Javed, K. Ahmad, I. Fatima, M. Safdar, N. Ashraf, A. Nadeem, Identification of phytochemicals as putative ligands for the targeted modulation of peroxisome proliferator-activated receptor α (PPAR α) in animals, *J. Biomol. Struct. Dyn.* 14 (2023) 1–12, <https://doi.org/10.1080/07391102.2023.2268185>.
- [48] J.K. Kim, I.J. Cho, E.O. Kim, D.G. Lee, D.H. Jung, S.H. Ki, S.K. Ku, S.C. Kim, Hemitepsin A inhibits T0901317-induced lipogenesis in the liver, *BMB Rep* 54 (2) (2021) 106–111, <https://doi.org/10.5483/BMBRep.2021.54.2.111>.
- [49] T. Huang, C.C. Zhao, M. Xue, Y.F. Cao, L.K. Chen, J.X. Chen, Y.J. Sun, J. Zeng, Current progress and outlook for Agrimonolide: a promising bioactive compound from *Agrimonia pilosa* Ledeb, *Pharmaceuticals* 16 (2) (2023) 150, <https://doi.org/10.3390/ph16020150>.
- [50] J.L.C.M. Dorne, M. Cirlini, J. Louise, L. Pedroni, G. Galaverna, L. Dellafiara, A computational understanding of inter-individual variability in CYP2D6 activity to investigate the impact of missense mutations on ochratoxin A metabolism, *Toxins* 14 (3) (2022) 207, <https://doi.org/10.3390/toxins14030207>.
- [51] C.A. González-Arias, S. Marín, A.E. Rojas-García, V. Sanchis, A.J. Ramos, UPLC-MS/MS analysis of ochratoxin A metabolites produced by Caco-2 and HepG2 cells in a co-culture system, *Food Chem. Toxicol.* 109 (Pt 1) (2017) 333–340, <https://doi.org/10.1016/j.fct.2017.09.011>.